Spinodal instability of suspensions of large spheres in a fluid of small spheres

1991 J. Phys.: Condens. Matter 3 F65

(http://iopscience.iop.org/0953-8984/3/42/006)

J. Phys.: Condens. Matter 3 (1991) F65–F72. Printed in the UK

Spinodal instability of suspensions of large spheres in a fluid of small spheres

Thierry Biben and Jean-Pierre Hansen

Laboratoire de Physique, Ecole Normale Supérieure de Lyon, 69364 Lyon, Cédex 07, France

Received 10 June 1991

Abstract. Numerical solutions of the thermodynamically self-consistent RY integral equation for the pair structure of a binary fluid hard sphere mixture, of size ratio $\sigma_1/\sigma_2 = 0.1$, exhibit divergent concentration fluctuations when the partial packing fractions of the two species are comparable, i.e. at low concentration of large spheres. This spinodal instability is studied at constant pressure, and it is shown that phase separation sets in for a reduced pressure $P^* = P\sigma_1^3/k_BT$ in the range $10^{-2} < P^* < 10^{-1}$.

1. Introduction

Charge or sterically stabilized suspensions of mesoscopic colloidal particles in a solvent share many common features with simple atomic liquids (for a recent review see [1]). While the dynamical properties, like the diffusion of the colloidal particles, are clearly affected by the presence of the solvent, experimental data on the spatial structure and the phase diagram of the suspension are generally interpreted on the basis of statistical models which ignore the microscopic nature of the suspending liquid. This point of view is usually justified by invoking the considerable difference in the length and time scales between the mesoscopic colloids and the microscopic solvent atoms, which naturally leads to a continuum picture of the latter. The current article is devoted to a 'discrete solvent' model of colloidal suspensions, namely a highly asymmetric binary mixture of hard spheres. In a preliminary publication [2] strong evidence was offered for fluid–fluid phase separation when the size ratio becomes sufficiently asymmetric. The calculations in [2] were carried out with a constant effective packing fraction of the small (solvent) spheres. In this article the stability limit, corresponding to the spinodal line, is investigated at constant pressure, and a rough estimate is obtained for the critical pressure P_c below which no phase separation occurs.

2. The asymmetric binary hard sphere model

The model under consideration is a binary mixture of hard spheres. The mixture contains ρ_1 'solvent' spheres per unit volume, of diameter σ_1 and ρ_2 'colloidal' spheres per unit volume, of diameter $\sigma_2 > \sigma_1$. Let $y = \sigma_1/\sigma_2 < 1$ be the size ratio and $\eta_\alpha = \pi\rho_\alpha\sigma_\alpha^3/6$ the partial packing fractions ($\alpha = 1, 2$). The diameters are assumed to

0953-8984/91/420F65+08$03.50

be additive throughout, i.e. $\sigma_{12} = (\sigma_1 + \sigma_2)/2$ and the focus will be on the situation where $y \ll 1$ but $\eta_1 \simeq \eta_2$, corresponding to concentrated colloidal suspensions. Under these conditions the number concentrations $x_1 = \eta_1/(\eta_1 + \eta_2 y^3)$ and $x_2 = \eta_2 y^3/(\eta_1 + \eta_2 y^3)$ are such that $x_2 \ll x_1 \simeq 1$. Since the temperature is an irrelevant variable for hard sphere systems, an equilibrium thermodynamic state of a binary mixture is entirely characterized by two independent variables which may be chosen to be the partial packing fractions η_1 and η_2 or any combination thereof (e.g. $\eta = \eta_1 + \eta_2$ and x_2). Alternatively one may choose as independent variables the reduced pressure $P^* = P\sigma_1^3/k_B T$ and η_2. Note that a straightforward application of Gibbs' phase rule to the present case allows at most three phases to coexist at a triple point.

The known results on binary hard sphere mixtures may be briefly summarized as follows. An analytic solution of the Percus–Yevick (PY) integral equations has been obtained in closed form [3] and shown to predict complete miscibility for hard sphere mixtures at all compositions and for all size ratios y [4]. The PY results exhibit the familiar thermodynamic inconsistency, in that the equation-of-state calculated from the virial theorem

$$\frac{\beta P}{\rho} = 1 + \frac{2\pi\rho}{3} \sum_{\alpha} \sum_{\beta} x_\alpha x_\beta \sigma_{\alpha\beta}^3 g_{\alpha\beta}(\sigma_{\alpha\beta}) \tag{1}$$

and from the compressibility relation

$$\left(\frac{\partial \beta P}{\partial \rho_\alpha}\right)_{\rho_\alpha} = 1 - \sum_{\beta} \rho_\beta \hat{c}_{\alpha\beta}(k=0) \tag{2}$$

differ by typically 20% at high packing fractions. In equation (1) the $g_{\alpha\beta}(\sigma_{\alpha\beta})$ are the contact values of the pair distribution functions, while in equation (2) $\hat{c}_{\alpha\beta}(k)$ denotes the Fourier transform of the $\alpha\beta$ direct correlation function ($1 \leqslant \alpha, \beta \leqslant 2$). If P_V denotes the pressure derived from (1) while P_C is the pressure calculated from (2) within the PY approximation, the linear combination [5]

$$P_M = \tfrac{1}{3} P_V + \tfrac{2}{3} P_C \tag{3}$$

yields results in good agreement with the available simulation data [6, 7]. The latter have been mostly limited to equimolar mixtures ($x_1 \simeq x_2$, and hence $\eta_1 \ll \eta_2$ when $y \ll 1$) and show no indication of phase separation, in qualitative agreement with the PY theory. An attempt to simulate moderately asymmetric mixtures ($y = \frac{1}{2}$ and $\frac{1}{3}$) with comparable packing fractions ($\eta_1 \simeq \eta_2$) met with considerable ergodicity problems [8] but again confirms the overall validity of the semi-empirical ansatz (3).

The fluid–solid phase diagram of weakly asymmetric hard sphere mixtures has been calculated from density functional theory [9] and from extensive Monte Carlo calculations of the free energy of substitutionally disordered hard sphere crystals [10]. The phase diagram exhibits a eutectic and phase separation in the solid phase for size ratios $y \lesssim 0.85$.

A striking feature of asymmetric hard sphere mixtures which is already apparent at the PY level [11, 12] is the 'osmotic depletion' effect which leads to an effective attraction (or 'stickiness') between the large spheres when their mutual distance is in the range $\sigma_2 \lesssim r \lesssim \sigma_1 + \sigma_2$. When $y \ll 1$, but $\eta_1 \simeq \eta_2$, the internal pressure is almost entirely due to the small (solvent) spheres; when these are expelled from the

volume left between two approaching large spheres, the pressure exerted by the solvent spheres on the diametrically opposite sides of the large spheres is no longer balanced, leading to a strong attractive interaction of entropic origin, and a contact value $g_{22}(\sigma_2)$ which diverges like $1/y$ in the PY approximation [12]. The effective attraction is a consequence of the discrete nature of the solvent and points to the inadequacy of the continuum picture of colloidal suspensions even in the limit $y \to 0$, the partial packing fractions being held constant. In [2] it was shown that the stickiness effect is enhanced when more accurate integral equations are used to determine the pair structure and that the resulting tendency towards aggregation of the large spheres leads to divergent concentration fluctuations and spinodal instability for size ratios $y \lesssim 0.2$. This aggregation phenomenon is very similar to 'depletion flocculation' as observed, for example, in recent simulations of asymmetric binary hard disk systems [13].

3. Numerical solutions of thermodynamically self-consistent integral equations

The predictions in [2] are based on numerical solutions of thermodynamically self-consistent integral equations. The latter are designed to enforce consistency between the virial and compressibility routes to the equation-of-state by the use of generalized closure relations containing parameters which are adjusted to that purpose. In [2] the closure proposed by Rogers and Young (RY) [14] and by Ballone *et al* (BPGG) [15] were used. Both closures lead to spinodal instability, although the divergence of concentration fluctuations is stronger with the RY closure. Since one- and two-parameter versions of the latter lead to similar results, we have more confidence in the RY closure and this will be adopted throughout this article. For the hard sphere mixture, the RY closure reads

$$g_{\alpha\beta}(r) = \Theta(r - \sigma_{\alpha\beta}) \left[1 + \frac{\exp(\gamma_{\alpha\beta}(r) f_{\alpha\beta}(r)) - 1}{f_{\alpha\beta}(r)} \right] \tag{4}$$

where Θ denotes the Heaviside step function, $\gamma_{\alpha\beta}(r) = h_{\alpha\beta}(r) - c_{\alpha\beta}(r)$ and $f_{\alpha\beta}(r)$ is a set of switching functions. The latter are chosen to be of the form

$$f_{\alpha\beta}(r) = 1 - \exp(-\xi_{\alpha\beta} r) \tag{5}$$

so that the closure (4) interpolates continuously between the familiar PY and hypernetted chain (HNC) closures when the parameters $\xi_{\alpha\beta}$ are varied from 0 to ∞. For any choice of $\xi_{\alpha\beta}$, the closure relation (4) together with the Ornstein–Zernike relations between the Fourier transforms of the total and direct correlation functions $h_{\alpha\beta}$ and $c_{\alpha\beta}$:

$$\hat{h}_{\alpha\beta}(k) = \hat{c}_{\alpha\beta}(k) + \sum_{\gamma} x_\gamma \hat{c}_{\alpha\gamma}(k) \hat{h}_{\gamma\beta}(k) \tag{6}$$

form a closed set of equations which were solved numerically using Gillan's hybrid algorithm [16]. The $\xi_{\alpha\beta}$ in (5) were assumed to be of the simple scaling form $\xi_{\alpha\beta} = \xi/\sigma_{\alpha\beta}$, and the single parameter ξ was adjusted until the total compressibilities calculated

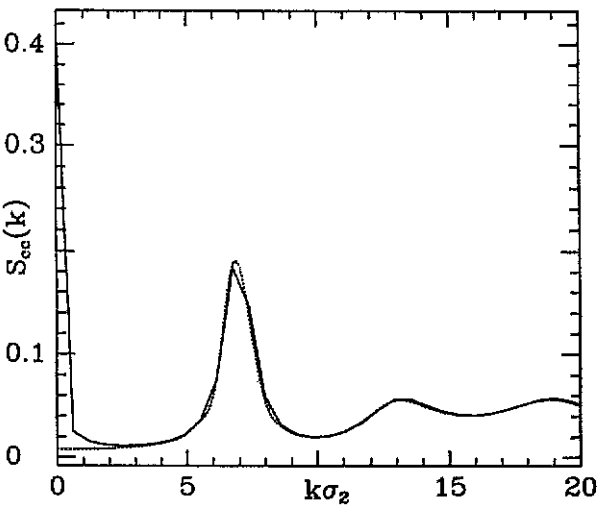

Figure 1. Concentration–concentration structure factor $S_{cc}(k)$ against $k\sigma_2$, for $y = 0.1$, $\eta_1 = 0.01$ and $\eta_2 = 0.5$: full curve, RY results; dots, PY results.

from equations (1) and (2) agreed to within better than 1%. This thermodynamic consistency could be achieved for all thermodynamic states investigated, except in the immediate vicinity of the spinodal line, where the concentration fluctuation diverges and thermodynamic consistency could only be aproximately satisfied in certain cases.

In [2] it was shown that an improved version of the RY equation (RY2) [17] which allows for independent variation of two $\xi_{\alpha\beta}$ parameters to satisfy the two thermodynamic consistency conditions associated with the partial (rather than the total) compressibilities, leads to results in good agreement with those obtained with the single parameter version described earlier. Consequently restriction will be made to the latter in the following. The key diagnostic signalling thermodynamic instability of a homogeneous mixture is provided by the divergence of concentration fluctuations. Let $\rho_{\boldsymbol{k}_\alpha}$ denote a Fourier component of the microscopic density of α-spheres:

$$\rho_{\boldsymbol{k}_\alpha} = \sum_{i=1}^{N\alpha} \exp(\mathrm{i}\boldsymbol{k}\cdot\boldsymbol{r}_{i\alpha}) \tag{7}$$

where $\boldsymbol{r}_{i\alpha}$ is the position of the ith sphere of species α. The local variable associated with concentration fluctuations is [18]

$$\rho_{\boldsymbol{k}_c} = x_2\rho_{\boldsymbol{k}_1} - x_1\rho_{\boldsymbol{k}_2} \tag{8}$$

and the corresponding concentration–concentration structure factor is

$$S_{cc}(k) = \tfrac{1}{N}\langle\rho_{\boldsymbol{k}_c}\rho_{-\boldsymbol{k}_c}\rangle \tag{9}$$

Standard fluctuation theory leads to the following long wavelength limit [18]

$$\lim_{k\to 0} S_{cc}(k) = \frac{Nk_BT}{(\partial^2 G/\partial x_1^2)_{N,P,T}} \tag{10}$$

where G denotes the Gibbs free energy, which turns from a concave to a convex function of the concentration x_1 on the spinodal, so that the diagnostic for the location of the latter is in the $k = 0$ divergence of the concentration–concentration structure factor, as calculated from the integral equation.

A typical example of PY and RY results for $S_{cc}(k)$ of a concentrated suspension with size ratio $y = 0.1$ is shown in figure 1. While the PY structure factor is very flat near the origin, indicative of very reduced concentration fluctuations, the latter are seen to be strongly enhanced within the thermodynamically self-consistent RY scheme, as signalled by a pronounced central peak in $S_{cc}(k)$.

4. Constant pressure results

In [2] the points of thermodynamic instability corresponding to divergent concentration fluctuations (spinodal points) were located by varying η_2 at constant *effective* packing fraction η_1' of the small (solvent) spheres. η_1' is determined by the volume $V' < V$ left by the large spheres, and accessible to the centres of the small spheres. In the limit $y \to 0$, $\eta_1' = \eta_1/(1-\eta_2)$, but the finite values of y, V' (and hence η_1') may be estimated from scaled particle theory [19].

Fixing η_1' is expected to be equivalent to working at constant pressure, at least in the limit $y \ll 1$, when the pressure is almost entirely determined by the fluid of small spheres. However, even for the smallest ratio explored in [2], namely $y = 0.1$, it was found that the pressure decreased significantly as η_2 was increased at fixed η_1'. On the other hand the pressures calculated from the RY closure agree systematically within better than 1%, with the predictions of the semi-empirical equation-of-state (3). Since the latter is a simple, analytic function of η_1 and η_2, it is easily inverted to yield the value of η_1 corresponding to given values of P^* and η_2. In this way approximately constant pressure calculations were carried out by solving

$$P_M^*(\eta_1, \eta_2) = P^* \tag{11}$$

for reduced pressures in the range $0.5 \geqslant P^* \geqslant 0.01$, and successive values of η_2. The resulting RY pressures are plotted in figure 2 as a function of η_2; they are seen to be very nearly constant and equal to the input value P^* in (11), and to decrease slightly for the largest values of $\eta_2 (\eta_2 \gtrsim 0.4)$. The variation of η_1 with η_2 is shown in figure 3.

Following the procedure summarized by equation (11) we are now in a position to investigate the thermodynamic stability of asymmetric binary hard sphere mixtures at (nearly) constant pressure. The calculations reported in [2] were carried out for large effective packing fractions $\eta_1' (\geqslant 0.4)$ of the solvent, corresponding to relatively high reduced pressures, $P^* \simeq 5$. For the size ratio $y = 0.1$, the spinodal was reached at a fairly low packing fraction of large spheres, $\eta_2 \simeq 0.05$. In an attempt to locate the critical point at the top of the spinodal curve, the present constant pressure calculations were carried out at much lower values of P^*, namely $0.01 \leqslant P^* \leqslant 0.5$. The variation of

$$\Lambda = \frac{x_1 x_2}{S_{cc}(k=0)} \tag{12}$$

with $x_2^{1/3}$ is shown in figure 4 for several pressures. For an ideal mixture or in the infinite dilution limit ($x_2 \to 0$ or 1) Λ goes to 1, while Λ drops to zero on the spinodal curve.

For $P^* = 0.01$ Λ is seen always to exceed 1, and to go through a maximum as a function of x_2 signalling complete miscibility at all concentrations. When $P^* \geqslant 0.1$, Λ first increases with η_2, goes through a maximum and then drops sharply to zero.

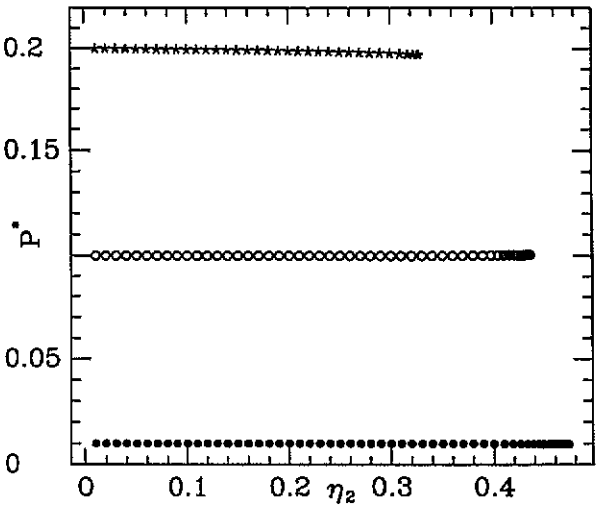

Figure 2. Reduced pressure P^*, as calculated from RY theory, plotted against η_2, for values of the estimate (3) of the pressure fixed at 0.2 (stars), 0.1 (open circles) and 0.01 (dots). The nearly horizontal behaviour proves that the present calculations correspond effectively to constant pressure.

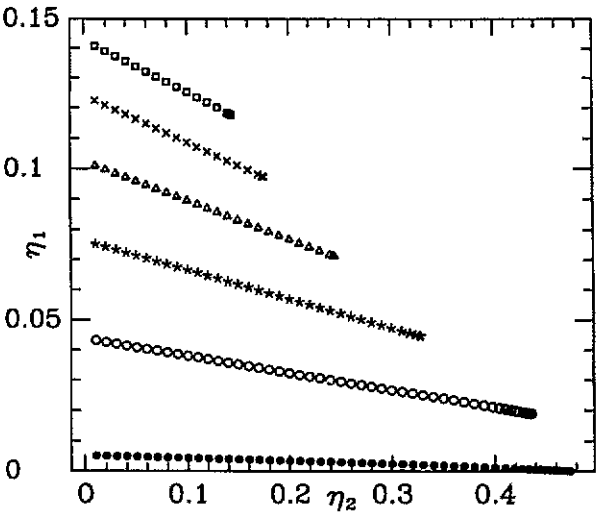

Figure 3. Variations of η_1 with η_2 for $P^* = 0.5$ (squares), 0.4 (crosses), 0.3 (triangles), 0.2 (stars), 0.1 (open circles) and 0.01 (dots).

Although numerical difficulties linked to the underlying divergence prevent solutions being obtained very close to the spinodal, the slope of the $\Lambda(\eta_2)$ curves becomes nearly vertical, leaving little doubt that they are headed towards zero. As P^* increases, the critical η_2 shifts towards smaller values as one might expect.

According to the results summarized in figure 4, the critical pressure P_c, below which no phase separation occurs, must be in the range $0.01 < P^* < 0.1$. Preliminary calculations carried out at pressures in that interval show indications of loops in the Λ plotted against $x_2^{1/3}$ curves, including regions where Λ goes negative, typical of

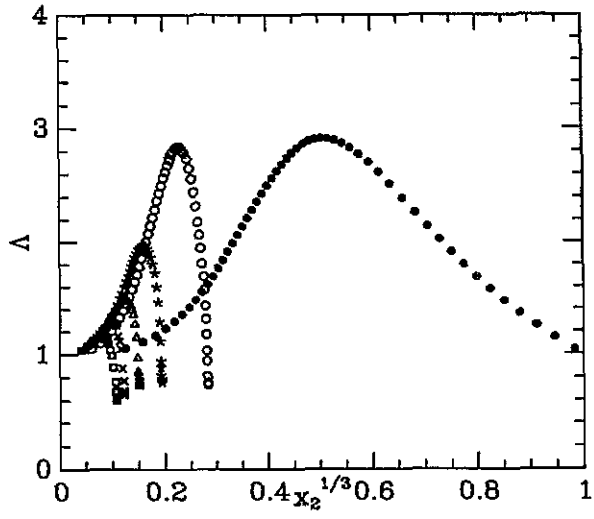

Figure 4. Λ (defined by (12)) plotted against $x_2^{1/3}$ for various pressures P^*. The symbols have the same meaning as in figure 3.

spinodal decomposition. More work in that part of the parameter space is in progress.

5. Discussion

The constant pressure results presented in this article confirm and extend the preliminary results of [2] which were carried out at constant effective packing fraction η_1'. Beyond a P^*-dependent critical concentration x_2 of large spheres, the binary mixture becomes unstable against concentration-fluctuations for a size ratio $y = 0.1$. Below a critical pressure P_c^* in the interval [0.01, 0.1], the binary hard sphere mixture is stable at all concentrations. Above P_c^* phase separation sets in. The present calculations predict the value of the maximum concentration of large spheres, but do not yield any information on the composition of the co-existing phase, which could be fluid or solid, with a higher concentration of large spheres. Another possibility would be a super-ionic-like phase, with the large spheres forming a close-packed crystal, while the small spheres could form a fluid within the interstitial space left by the large spheres.

Although we are far from being able to present a complete phase diagram, the present calculations which supplement those of [2] show that fluid mixtures of hard spheres are unstable against phase separation, for sufficiently asymmetric size ratios.

Although a direct check of the predictions based on the self-consistent integral equations by computer simulation is not an easy task, as pointed out already in section 2, an attempt to observe fluid–fluid phase coexistence in highly asymmetric hard disk and hard sphere mixtures will be made using the Gibbs ensemble and a generalization of the 'particle swapping' technique [20].

Acknowledgments

The authors are indebted to Giorgio Pastore for making his efficient integral equation code available and to Daan Frenkel for helpful comments.

References

[1] Pusey P N 1991 *Liquids, Freezing and the Glass Transition* ed J P Hansen, D Levesque and J Zinn-Justin (Amsterdam: North-Holland) p 763
[2] Biben T and Hansen J-P 1991 *Phys. Rev. Lett.* **66** 2215
[3] Lebowitz J L 1964 *Phys. Rev.* A **133** 895
[4] Lebowitz J L and Rowlinson J S 1964 *J. Chem. Phys.* **41** 133
[5] Mansoori G A, Carnahan N F, Starling K E and Leland T W 1971 *J. Chem. Phys.* **54** 1523
[6] Alder B J 1964 *J. Chem. Phys.* **40** 2724
[7] Jackson G, Rowlinson J S and van Swol F 1987 *J. Chem. Phys.* **91** 4907
[8] Fries P and Hansen J-P 1983 *Mol. Phys.* **48** 891
[9] Barrat J L, Baus M and Hansen J-P 1986 *Phys. Rev. Lett.* **56** 1063
[10] Kranendonk W G T and Frenkel D 1991 *Mol. Phys.* **72** 679 and 699
[11] Henderson D 1988 *J. Colloid. Interface Sci.* **121** 486
[12] Biben T and Hansen J-P 1990 *Europhys. Lett.* **12** 347
[13] Dickinson E 1989 *J. Colloid. Interface Sci.* **132** 274
[14] Rogers F J and Young D A 1984 *Phys. Rev.* A **30** 999
[15] Ballone P, Pastore G, Galli G and Gazzillo D 1986 *Mol. Phys.* **59** 275
[16] Gillan M J 1979 *Mol. Phys.* **38** 1781
[17] Bernu B, Hansen J-P, Hiwatari Y and Pastore G 1987 *Phys. Rev.* A **36** 4891
[18] Bhatia A B and Thornton D E 1970 *Phys. Rev.* B **2** 3004
[19] Lebowitz J L, Helfand E and Praestgaard E 1965 *J. Chem. Phys.* **43** 774
[20] Panagiotopoulos A Z 1989 *Int. J. Thermophys.* **10** 447